

Supplementary Information

A High-Performance Magnetoelectric Non-Volatile Light-Emitting Memory

Jia-Wei Wu^a, Yu-Chieh Chao^a, Jia-Yu Lin^a, Chia-Chun Ho^a, Meng-Ching Lai^a, Fang-Chi Hsu^{b,*} and Yang-Fang Chen^{a,*}

^aDepartment of Physics, National Taiwan University, Taipei 106, Taiwan.

^bDepartment of Materials Science and Engineering, National United University, Miaoli 360, Taiwan.

Contents

S1. Characterization of the RRAM

S2. Characterization of the magnetoelectric device

S3. SEM image of the integrated RRAM-QLED device

S4. J - V curves of the integrated RRAM-magnetoelectric device

S5. Cyclic J - V and E - V Characterization of the magnetoelectric LEM

S6. Performance of QLEDs using ITO of different surface roughness

S1. Characterization of RRAM

Here, we demonstrate the performance of ITO/PMMA/Ag RRAM. The working area of the RRAM cell is defined as the overlapping area between the ITO electrode and the Ag electrode, which is 0.04 cm^2 . When characterizing the performance of the RRAM cell, the ITO electrode is grounded and the Ag electrode is biased. Figure S1a shows the J - V characteristics of the RRAM cell. The J - V curve steeply increases at $+1.1 \text{ V}$ and suddenly drops at -1.3 V . When the voltage surpasses $+1.1 \text{ V}$, the RRAM cell switches its state from the HRS to the LRS. At the LRS, the compliance current density is set to 1.25 mA cm^{-2} . When the negative bias exceeds -1.3 V , the RRAM cell switches from the LRS to the HRS. The ON/OFF ratio is defined as the current ratio of the LRS to the HRS, which reaches about 10^3 . However, the performances of RRAM cells fluctuate in every single device.^{S1} The statistical results for set and reset voltages are $(+1.37 \pm 0.34) \text{ V}$ and $(-1.88 \pm 0.38) \text{ V}$, respectively. Figure S1b shows the ON/OFF ratio of the RRAM cell at a reading voltage of $+0.1 \text{ V}$ for 50 cycles. The ON/OFF ratio keeps at 10^3 for 50 cycles, which exhibits phenomenal reading performance for memory devices.^{S2} In this work, the structure of the RRAM cell in the magnetically controllable LEM device is the Au/PMMA/Ag structure. The ITO electrode is replaced by the Au electrode, which does not affect the performances of the devices.

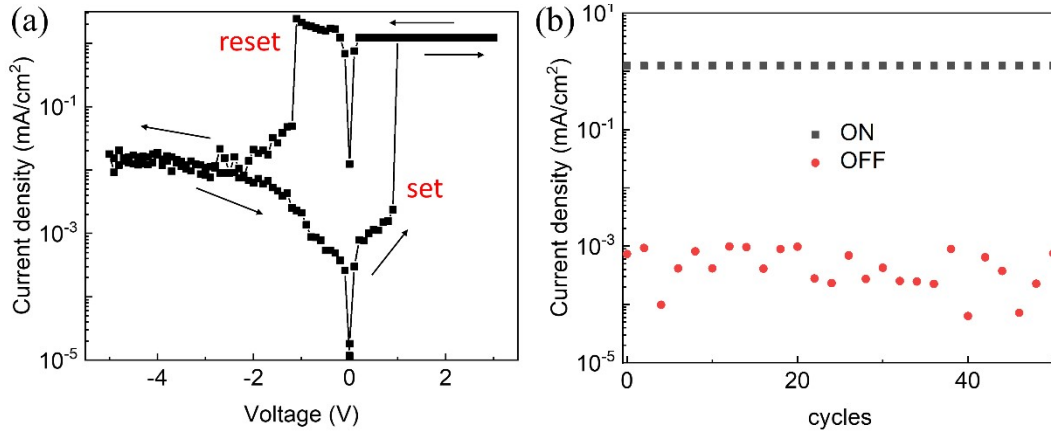


Fig. S1 Device performance of the ITO/PMMA/Ag RRAM. (a) J - V characteristics of the ITO/PMMA/Ag RRAM. (b) ON/OFF switching for 50 cycles of the ITO/PMMA/Ag RRAM at a reading voltage of +0.1 V.

S2. Characterization of the magnetoelectric device

The current response of the magnetoelectric device with respect to magnetic fields at the reading voltage of +0.1 V is shown in Figure S2a. From 0 mT to 52 mT, the magnetoelectric device is not activated because the magnetic film does not contact with the bottom electrode. When the magnetic field exceeds 52 mT, the output current increases rapidly due to the large contact area between the magnetic film and the bottom electrode. As further increasing the field strength, the current saturates because the contact area reaches the maximum. The threshold field is 52 mT and the corresponding current output, I_0 , is 2.28×10^{-8} (A). For a more clear understanding of the current response with the magnetic field, we defined the sensitivity, S , as $S = (\Delta I/I_0)/\Delta B$,^{S3}

where ΔI is the change in current, and ΔB is the change in magnetic field and the result is shown in Figure S2b. The sensitivity is divided into three regions: the low-magnetic field region (<52 mT), the high-sensitivity region (52-172 mT), and the saturation region (>172 mT), with sensitivities of $1.53\% \text{ mT}^{-1}$, $5282.01\% \text{ mT}^{-1}$, and $622.65\% \text{ mT}^{-1}$, respectively

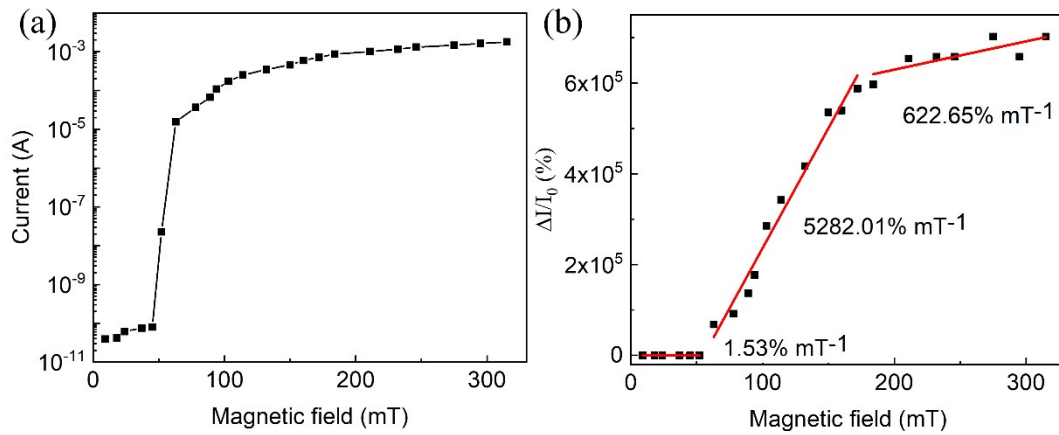


Fig. S2 Characterization of the magnetoelectric device. (a) Current response of the magnetoelectric device with respect to magnetic fields at a working voltage of +0.1 V. (b) Sensitivity of the magnetoelectric device at a reading voltage of +0.1 V.

S3. SEM image of the integrated RRAM-QLED device

Figure S3 shows the SEM image of the integrated RRAM-QLED device. Note that the thickness of the self-assembled monolayer (P3HT-COOH) is only about 1 nm,^{S4} which is unlikely to be clearly observed in the SEM image.

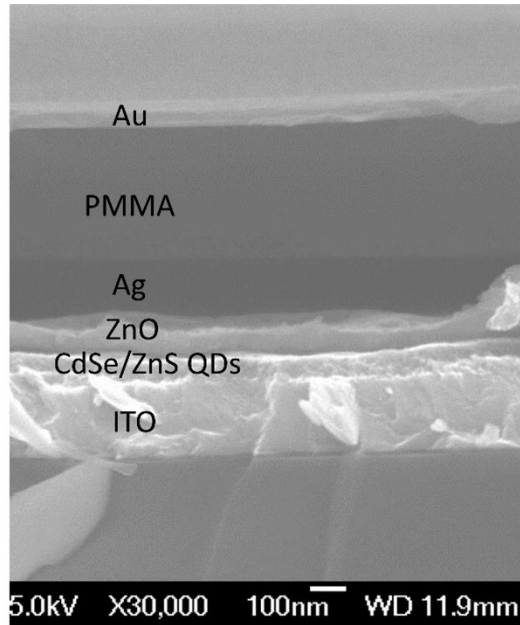


Fig. S3 SEM image of the integrated RRAM-QLED device (Ag/PMMA/Au RRAM and the ITO/P3HT-COOH/CdSe/ZnS QDs/ZnO/Ag QLED).

S4. J - V curves of the integrated RRAM-magnetoelectric device

The integrated device of RRAM and magnetoelectric device behaves as a dual-gate transistor. The J - V characteristics under various magnetic field strengths are shown in Figure S5. The set and reset voltages increase as the applied magnetic fields decrease. The SET/RESET voltages are +1.3/-1.5 V, +1.6/-1.9 V and +2.2/-2.3 V at 338, 273, and 145 mT, respectively.

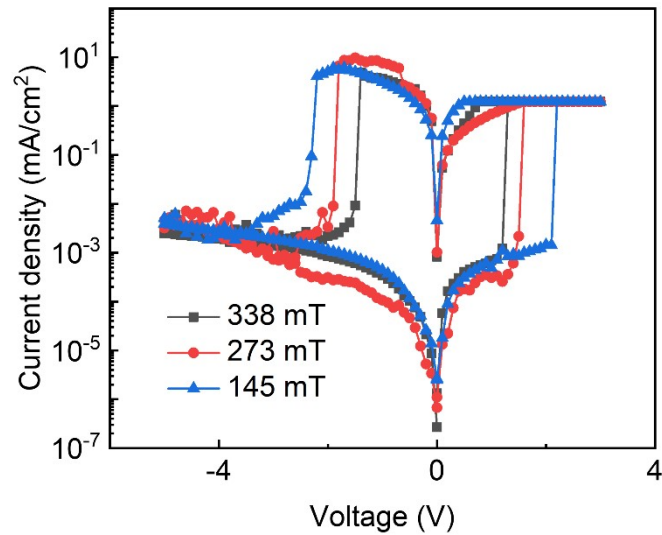


Fig. S4 J - V characteristic of RRAM integrated with magnetoelectric device under different magnetic field strengths.

S5. Cyclic $J - V$ and $E - V$ Characterization of the magnetoelectric LEM

Figure S5(a) depicts the cyclic $J - V$ sweep curves between 0 and +6V at 250 mT and the statistical value for the SET voltage is $+(3.28 \pm 0.148)$ V. Figure S5(b) shows the variation of EL intensity in the forward ($0 \sim +6$ V) and the reverse voltage sweeps ($+6 \sim 0$ V) under different magnetic field strengths. During the first sweep ($0 \sim +6$ V), the magnetoelectric LEM starts in the HRS. The emitting light appears when the applied voltage exceeds the turn-on voltage, and the EL intensity is limited by the compliance current of 5 mA. In the reverse sweep ($+6 \sim 0$ V), the EL intensity follows the upper curves. The higher intensity during the reverse sweep indicates that the magnetoelectric LEM is in the LRS.

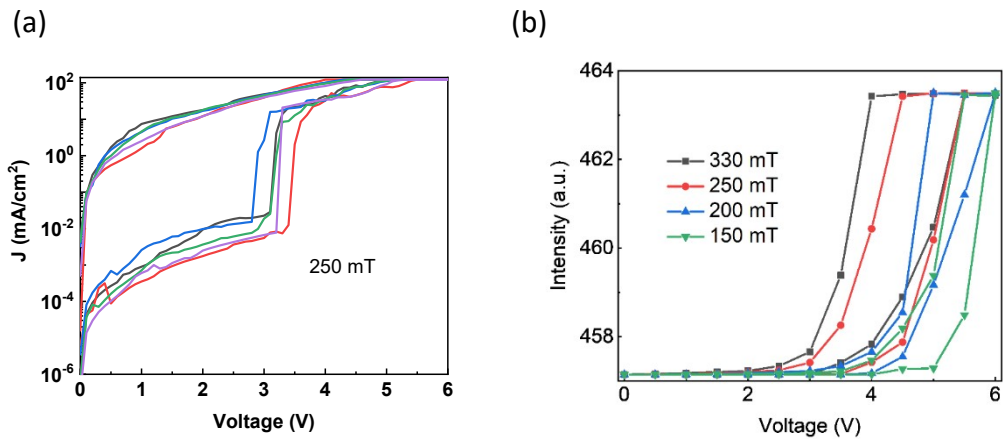


Fig. S5 (a) Cyclic $J - V$ sweep curves at 250 mT. (b) EL intensity of the magnetoelectric memory under different bias and magnetic field.

S6. Performance of QLEDs using ITO of different surface roughness

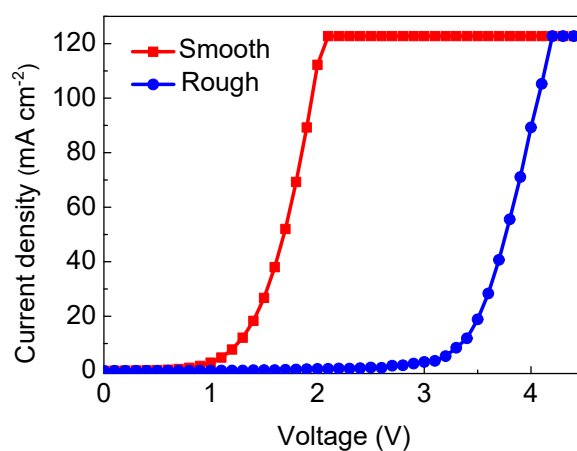


Figure S6. $J - V$ characteristics for QLEDs using smooth and rough ITO as electrodes.

Reference

- S1 F. Zahoor, T. Z. A. Zulkifli and F. A. Khanday, *Nanoscale Res. Lett.* **2020**, 15, 90.
- S2 N. Raeis-Hosseini, D. G. Georgiadou and C. Papavassiliou, *ACS Appl. Electron. Mater.* **2023**, 5, 138-154.
- S3 Y. Zang, F. Zhang, D. Huang, C.-A. Di and D. Zhu, *Adv. Mater.* **2015**, 27, 7979-7985.
- S4 C.-Y. Chang, H.-H. Huang, H. Tsai, S.-L. Lin, P.-H. Liu, W. Chen, F.-C. Hsu, W. Nie, Y.-F. Chen and L. Wang, *Adv. Sci.* **2021**, 8, 2002718.